

Tailoring of High-Order Multiple Emulsions by the Liquid–Liquid Phase Separation of Ternary Mixtures**

Martin F. Haase* and Jasna Brujic*

Abstract: Multiple emulsions with an “onion” topology are useful vehicles for drug delivery, biochemical assays, and templating materials. They can be assembled by ternary liquid phase separation by microfluidics, but the control over their design is limited because the mechanism for their creation is unknown. Herein we show that phase separation occurs through self-similar cycles of mass transfer, spinodal decomposition or nucleation, and coalescence into multiple layers. Mapping out the phase diagram shows a linear relationship between the diameters of concentric layers, the slope of which depends on the initial ternary composition and the molecular weight of the surfactant. These general rules quantitatively predict the number of droplet layers (multiplicity), which we used to devise self-assembly routes for polymer capsules and liposomes. Moreover, we extended the technique to the assembly of lipid-stabilized droplets with ordered internal structures.

Multiple emulsions consist of droplets that encapsulate layers of oil and water from the continuous phase.^[1] An active ingredient can be sequestered inside the inner droplets and subsequently released. The layering inside the droplets allows for the release of active ingredients in consecutive steps over long periods of time.^[2,3] Control over the internal structure makes multiple emulsions much sought after in the pharmaceutical, cosmetic, and food industries.^[4] These emulsions offer versatile templates for structured and patchy colloids,^[5,6] particles of programmable shape,^[7] self-assembly tools,^[8,9] and biomaterials.^[10] The use of PDMS microfluidics with multiple channels^[11] or glass capillaries with combined flows^[12–15] enables the mechanical construction of high-order multiple emulsions. Furthermore, the use of single surfactants that can stabilize both oil-in-water and water-in-oil layers simplifies their synthesis.^[16] These techniques are unsuitable for large-scale production because the number and size of the inner layers are determined by microfluidic flows. A simpler process that leads to the spontaneous formation of multiple emulsions consists of the liquid–liquid phase separation of

ternary mixtures.^[17–19] This method enables the stabilization of submicron double emulsions,^[20] which are difficult to construct mechanically. These recent results call for an understanding of the basic principles of phase separation inside emulsion droplets. In equilibrium, ternary liquid phase separation leads to double emulsions of pure oil and water. The slow rate of mass transfer enables local fluctuations in composition to seed multiple phase-separation events within a single droplet. These kinetic pathways control the emulsion layers and open the possibility of mass production because there is no need for surface patterning, multiple channels, and complex flow fields.

In this study, we investigated the quantitative dependence of the number and size of the inner droplets on the outer droplet size, the initial composition of the ternary mixture on the binodal line, and the molecular mass of the surfactant. We first visualized the formation of emulsion layers through a single channel flow to study the mechanism of phase separation. The whole process can be mapped onto a trajectory on the phase diagram from the miscible region to complete phase separation. These emulsions serve as precursors for other particulate materials, such as polymer capsules^[21–23] and lipid vesicles.^[2,24] We additionally show that the ternary mixture can be loaded with active ingredients for drug delivery. Finally, these high-order emulsions could be coalesced into a single droplet to give, for the first time, lipid-stabilized droplets with ordered structures.^[16,25,26]

Multiple emulsions are produced by dripping a single-phase ternary mixture of an oil, a polar solvent, and water through a microcapillary into a water stream containing a surfactant, as depicted in Figure 1 a (see also Figure S1 in the Supporting Information). As a model study, we used diethyl phthalate (DEP), ethanol, and water stabilized by the hydrophilic surfactant Pluronic F127 (0.1 wt %). The injection of a mixture close to the binodal line of the ternary phase diagram^[27] yields monodisperse, multiple high-order emulsions. The mutual solubility of water and DEP is negligible. To slow down the process from seconds in Figure 1 b to a minute (see Videos S1 in the Supporting Information) to visualize the formation of a quintuple droplet, we enlarge the microfluidic device tenfold and increase the viscosity of the continuous phase with polyalginate (0.5 wt %). This modification does not affect the phase behavior significantly. The initial composition of the injected ternary mixture governs droplet multiplicity, as shown in Figure 1 c. By increasing the water and ethanol content from composition (1) to (5) along the binodal line, the number of inner droplets can be increased incrementally up to five. However, a further increase reverses the trend, as shown by the triple and double emulsions at compositions (6) and (7), respectively.

[*] M. F. Haase, J. Brujic
Center for Soft Matter Research, Physics Department
New York University (USA)
E-mail: jb2929@nyu.edu

[**] This research was supported partially by the National Science Foundation MRSEC Program under Grant No. DMR-0820341 for material support and the Career Grant No. 0955621. We thank Eric Vanden-Eijnden, Jerome Bibette, and Raphael Blumenfeld for enlightening discussions. J.B. thanks Tuomas Knowles and Daan Frenkel for hosting her sabbatical at the University of Cambridge.



Supporting information for this article is available on the WWW under <http://dx.doi.org/10.1002/anie.201406040>.

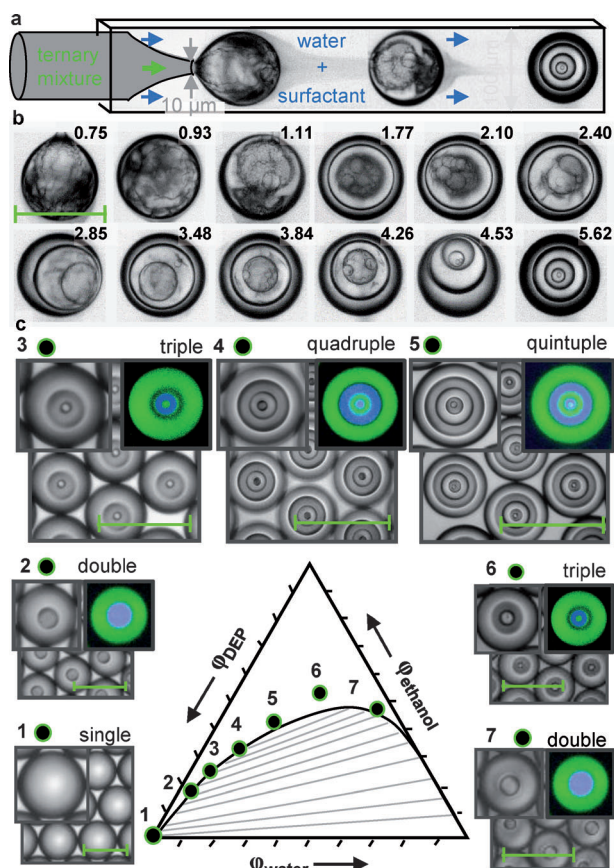


Figure 1. a) Schematic illustration of a microfluidic glass capillary. b) Formation of a quintuple droplet over time (in seconds) from a DEP/ethanol/water mixture (0.41/0.42/0.17 vol%). c) Ternary phase diagram showing the effect of composition on the multiplicity of the droplets as microscopic images for points (1–7) on the diagram. Fluorescein isothiocyanate (FITC) and Nile red dyes label water (blue) and oil layers (green), respectively. Scale bars are 100 μm .

These observations can be understood in terms of the mechanism of phase separation, as revealed by video microscopy. The phase separation of composition (5) is mapped onto a zigzag trajectory on the phase diagram in Figure 2. During droplet formation, mass transfer of ethanol and DEP occurs into the external water, whereas the exchange of water across the interface brings the surfactant in (Figure 2, stage 1). This mass transfer induces a compositional change in the mixture, which shifts it to a tie line in the immiscible region. Owing to the proximity of the measured binodal and postulated spinodal lines near the plait point, internal phase separation occurs through spinodal decomposition (Figure 2, stage 2). This process initially forms an outermost layer, which we conjecture is rich in DEP. This layer slows down the mass transfer of ethanol to the continuous phase and encases the inner droplet with the Pluronic surfactant (Figure 2, stage 3). Spinodal decomposition results in a double emulsion (Figure 2, stage 4) with compositions that are given by the tie line connecting the oil-rich (left) and the water-rich (right) side on the binodal curve. Nonequilibrium fluctuations in composition, driven by the

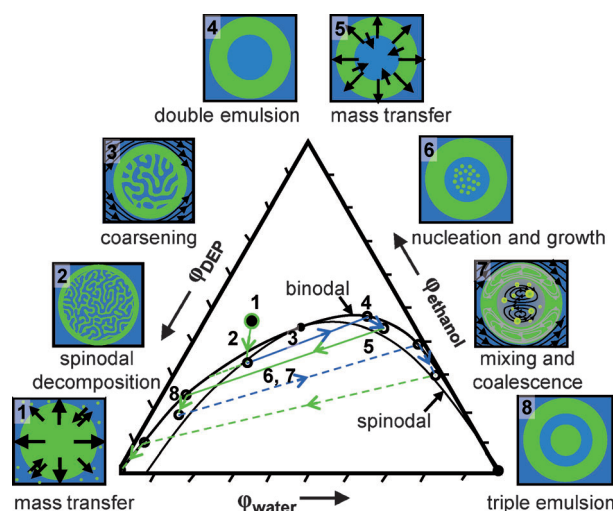


Figure 2. The blue and green zigzag trajectory follows the compositional evolution of the innermost droplet from the miscible region (1) to a triple emulsion (8), and continues until complete phase separation along the dashed line. Schematic diagrams illustrate the stages of phase-separation cycles.

removal of ethanol (Figure 2, stage 5) and the mixing induced by internal flows, seed a nucleation event inside the inner droplet (Figure 2, stage 6). This phase separation occurs along the next tie line through the nucleation and growth of small inner DEP droplets. The internal flow induces these droplets to mix (Figure 2, stage 7; see also the Supporting Information) and coalesce because the ethanol in the water-rich phase renders the Pluronic F127 surfactant inefficient. Further removal of ethanol stabilizes a triple emulsion (Figure 2, stage 8). Subsequent cycles of phase separation that form further inner layers occur through nucleation and growth, as does starting with a composition in this region (see Figure S2 and Video S1 c). The phase-separation process stops when there is no longer enough dissolved DEP and water available to form more droplets. These multiple emulsions are stable for weeks. Ternary mixtures of many other oils and polar solvents, such as acetic acid or propanol, can be used with similar results. However, more work is needed to measure the compositions during phase separation and to obtain quantitative evidence of the observed steps. Moreover, bulk emulsification of the ternary mixture through a membrane emulsifier^[28] gives large quantities of polydisperse emulsions with variable multiplicities as a result of inhomogeneities in the flow (see Figure S3).

As a general rule, the highest multiplicity is achieved with the ternary composition (on the oil-rich side) whose splitting along the tie line gives rise to an inner water droplet with the highest oil content. This composition maximizes the number of zigzag cycles and explains the increase in multiplicity from point (1) to point (5) in Figure 1 c, in which the tie line closest to point (5) yields droplets richest in DEP (20–30 vol%). The initial compositions at points (6) and (7) rapidly nucleate small DEP droplets that coalesce upon contact with the continuous phase, thus leaving less material behind for phase separation.

For a given ternary liquid composition and flow rate, the multiplicity depends on the ability of the surfactant to stabilize interfaces. In particular, the multiplicity in the example in Figure 1 increases with the molecular mass of the Pluronic surfactant (see Figure S4). A larger surfactant, such as F127, retains more DEP through steric inhibition of the coalescence of nucleated DEP droplets with the outer layer of the same type. These droplets preferentially coalesce with one another (see Videos S1) because the rapid loss of ethanol from the outer DEP layer improves surfactant stabilization at the interface. Also, mass transfer through a layer of a larger surfactant may be reduced, thus increasing multiplicity.

The number and diameter of the inner droplets also depend on the size, d_1 , of the outer droplet generated by the microfluidics. For the ternary composition at point (5) in Figure 1 c, the diameter d_j of the j th inner droplet is plotted in Figure 3 a as a function of d_1 for $j=2,3,4,5$. The resulting graphs reveal a linear relationship between d_j and d_1 , and also show that the diameter d_1 of the outer droplet controls the multiplicity of the inner droplets. For example, d_1 must be larger than $5.6 \mu\text{m}$ to create a doublet ($j=2$) and larger than $60 \mu\text{m}$ to create a quintuplet ($j=5$), as shown by the intercepts in Figure 3 a.

More importantly, Figure 3 b shows that all the data collapse onto a single linear master curve when consecutive layer diameters are plotted against each other, thus implying that the process is self-similar: d_{j+1} is to d_j as d_j is to d_{j-1} . This line is fitted by $d_{j+1} = a d_j - b$, with $a = 0.66$ and $b = 3.7 \mu\text{m}$, and it can be used to predict the multiplicity from the outer-droplet diameter d_1 . Starting from $d_{j+1} = d_j$, we count the number of phase-separation events down the staircase between the curves $d_{j+1} = a d_j - b$ and $d_{j+1} = d_j$ before crossing the threshold value $d_j = b/a = 5.6 \mu\text{m}$, below which no additional inner droplet can be created. This limit exists because smaller inner droplets dissolve in the oil as a result of their Laplace pressure. Since osmotic pressure counteracts the Laplace pressure of the inner drop, it is possible to decrease the size of the inner droplet down to the micron scale by applying an osmotic pressure to the droplets (see Figure S5). To precalculate the threshold values of d_1 at which the multiplicity increases, we can alternatively go up the staircase from $b/a = 5.6 \mu\text{m}$. By denoting these threshold values as D_n with $n=1,2,\dots$, this approach amounts to starting from $D_1 = b/a$ and solving $D_1 = b/a = a D_2 - b$ in D_2 to get $D_2 = b/a + b/a^2$ and so on, which gives:

$$D_n = \frac{b}{a} + \frac{b}{a^2} + \dots + \frac{b}{a^n} = \frac{b}{a^n} \frac{1 - a^n}{1 - a} \quad n = 1, 2, \dots$$

so that the final multiplicity will be $j = n + 1$ if $D_n \leq d_1 < D_{n+1}$, as shown by the dashed line in Figure 3 b. An increase in the initial volume fraction of water, ϕ_{water}^0 , for ternary compositions along the binodal line does not alter the linear law nor the value of the intercept ($b = (3.5 \pm 0.5) \mu\text{m}$), but does increase the slope a , as shown in Figure 3 c. A steeper slope implies tighter spacing between consecutive emulsion layers and therefore a higher multiplicity. In the inset in Figure 3 c,

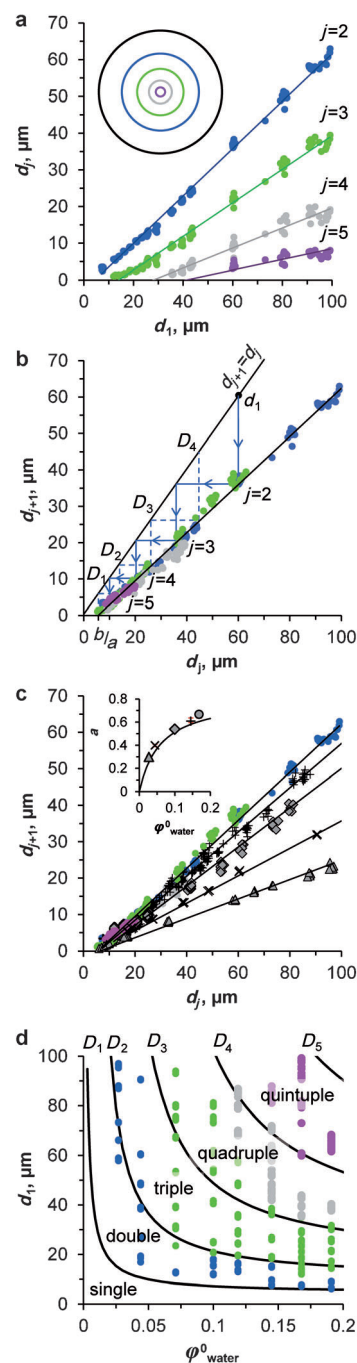


Figure 3. a) Linear dependence of the inner layer diameter d_j on the outer diameter d_1 . b) A plot of d_{j+1} as a function of the previous layer diameter d_j reveals a linear relationship with slope a . The intercept b gives the smallest double emulsion at b/a . The multiplicity is the number of steps between the line with slope 1 and the master curve (blue arrow line); the dashed line connects the values of D_n . c) The slope a increases with the initial water content on the binodal line, as shown by the fit in the inset. d) Isomultiplicity lines are in good agreement with the data.

we empirically fit $a = 0.84 \phi_{\text{water}}^0 / (0.065 + \phi_{\text{water}}^0)$, which enables us to predict the multiplicity thresholds D_n as a function of two experimental control parameters, the outer droplet size d_1 and ϕ_{water}^0 (Figure 3 d). These “isomultiplicity” lines capture the experimental multiplicities well, with the excep-

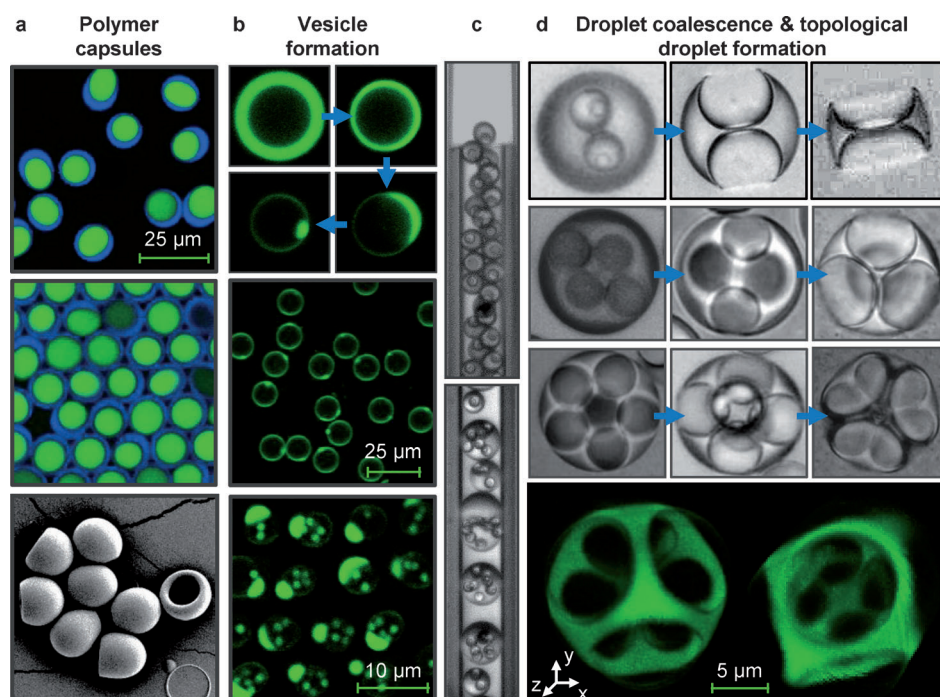


Figure 4. a) Double w/o/w emulsions, dyed with FITC (green) and Nile red (blue), become water-filled PMMA capsules that buckle upon drying. b) Top and middle: Assembly of fluorescently dyed lipids into unilamellar vesicles as the oil evaporates. Bottom: Vesicles loaded with 1 μm colloids. c) Coalescence of triple emulsions. d) Shape changes of multiple emulsions with 2, 4, and 6 water droplets (top, black and white) to give ordered inner structures (bottom, green). The snapshots of shape changes do not correspond to the same droplets.

tion of large droplets at low values of ϕ_{water}^0 , which tend to have fewer inner droplets than predicted. This overestimation is probably due to the inability of the surfactant to stabilize the innermost droplet owing to the decrease in the surfactant concentration towards the center of the droplet.

The liquid–liquid phase separation can be applied to other surface-active materials to construct distinct architectures. Of particular use in drug delivery is the encapsulation of molecules into water-filled biodegradable polymer shells. We empirically deduced the ternary composition of butyl acetate (BA)/ethanol/water, which phase separates into a double emulsion stabilized by Pluronic F127. When the water-insoluble polymer poly(methyl methacrylate) (PMMA) was dissolved into the ternary mixture, a solid PMMA capsule evolved upon the evaporation of volatile BA (Figure 4a). These capsules are deformed from a spherical shape by the buoyancy of the inner water and buckle on one side upon drying, as shown in the electron micrograph. Alternatively, the addition of phospholipids (e.g. 1,2-dioleoylphosphatidylcholine (DOPC)) to the same ternary mixture and Pluronic F127 yields monodisperse unilamellar vesicles (Figure 4b). The BA begins to evaporate and dewets from the nascent lipid bilayer into a cap, which then detaches to form a separate oil droplet. This process leaves behind lipid/block-copolymer vesicles, which can be loaded with active ingredients or colloidal particles in the initial ternary mixture (see Videos S2a).

Multiple emulsions can also be used to seed droplets with complex topologies. Lipids that stabilize water-in-oil but not

oil-in-water interfaces generate multiple emulsions with outermost oil layers that coalesce upon droplet contact (Figure 4c). In particular, we chose a ternary composition of chloroform/ethanol/water stabilized with DOPC and Pluronic F127 that phase separates into triple emulsions. Whereas the water layer is stabilized by DOPC, the inner oil droplet evaporates, and the outer oil layers coalesce because the Pluronic surfactant is soluble in chloroform. The concentration of these droplets in a microfluidic channel yields multiple emulsions with spatially separated droplets (see Figure S6 and Video S2b), which have only been constructed by forced emulsification.^[29] The subsequent evaporation of 70–90% of the volume of chloroform from the outer layer changes the droplet shape into a unique geometry, which depends on the number of inner droplets, as shown in the examples in Figure 4d (see Vid-

eos S2c). This result is analogous to the symmetry observed in colloidal clusters,^[30] except that the shape of the outer droplet is supported by bilayers between the inner water droplets and either the continuous phase or the chloroform layer. Confocal images reveal two views of the internal structure of a chloroform droplet consisting of six water droplets. If these liquid structures can be solidified in future work, they could be used as compartments for biochemical reactions. These complex topologies are similar to those of microcapsules,^[31] but are stabilized by phospholipid scaffolds.

Received: June 9, 2014

Revised: August 6, 2014

Published online: September 8, 2014

Keywords: microfluidics · multiple emulsions · phase diagrams · phase separation · surfactants

[1] L. Y. Chu, A. S. Utada, R. K. Shah, J. W. Kim, D. A. Weitz, *Angew. Chem. Int. Ed.* **2007**, *46*, 4944–4947; *Angew. Chem.* **2007**, *119*, 5032–5035; L.-Q. Chu, R. Förch, W. Knoll, *Angew. Chem. Int. Ed.* **2007**, *46*, 4944–4947; *Angew. Chem.* **2007**, *119*, 5032–5035.

[2] S. H. Kim, J. W. Kim, J. C. Cho, D. A. Weitz, *Lab Chip* **2011**, *11*, 18.

[3] A. Abbaspourrad, N. J. Carroll, S. H. Kim, D. A. Weitz, *J. Am. Chem. Soc.* **2013**, *135*, 20.

[4] C. X. Zhao, *Adv. Drug Delivery Rev.* **2013**, *65*, 11.

[5] S. M. Yang, S. H. Kim, J. M. Lim, G. R. Yi, *J. Mater. Chem.* **2008**, *18*, 19.

- [6] G. R. Yi, D. J. Pine, S. Sacanna, *J. Phys. Condens. Matter* **2013**, *25*, 19.
- [7] S. Sacanna, M. Korpics, K. Rodriguez, L. Colón-Meléndez, S. H. Kim, D. J. Pine, G. R. Yi, *Nat. Commun.* **2013**, *4*, 1688.
- [8] L. Feng, L. L. Pontani, R. Dreyfus, P. Chaikin, J. Brujic, *Soft Matter* **2013**, *9*, 41.
- [9] M. Hadorn, E. Boenzli, K. T. Sørensen, H. Fellermann, P. E. Hotz, M. M. Hanczyc, *Proc. Natl. Acad. Sci. USA* **2012**, *109*, 20320–20325.
- [10] S. Mitragotri, J. Lahann, *Nat. Mater.* **2009**, *8*, 1.
- [11] A. R. Abate, D. A. Weitz, *Small* **2009**, *5*, 18.
- [12] S. H. Kim, D. A. Weitz, *Angew. Chem. Int. Ed.* **2011**, *50*, 12572–12577; *Angew. Chem.* **2011**, *123*, 12780–12785.
- [13] A. R. Abate, J. Thiele, M. Weinhart, D. A. Weitz, *Lab Chip* **2010**, *10*, 14.
- [14] F. Tu, D. Lee, *Langmuir* **2012**, *28*, 26.
- [15] N. N. Deng, W. Wang, X. J. Ju, R. Xie, D. A. Weitz, L. Y. Chu, *Lab Chip* **2013**, *13*, 20.
- [16] J. A. Hanson, C. B. Chang, S. M. Graves, Z. Li, T. G. Mason, T. J. Deming, *Nature* **2008**, *455*, 7209.
- [17] C. X. Zhao, A. P. Middelberg, *Angew. Chem. Int. Ed.* **2009**, *48*, 8729–8732; *Angew. Chem.* **2009**, *121*, 8885.
- [18] C. H. Choi, D. A. Weitz, C. S. Lee, *Adv. Mater.* **2013**, *25*, 18.
- [19] Y. Song, A. Sauret, H. C. Shum, *Biomicrofluidics* **2013**, *7*, 061301.
- [20] W. C. Jeong, M. Choi, C. H. Lim, S. M. Yang, *Lab Chip* **2012**, *12*, 24.
- [21] N. Zydowicz, E. Nzimba-Ganyanad, *Polym. Bull.* **2002**, *47*, 5.
- [22] H. C. Shum, Y. Zhao, S. Kim, D. A. Weitz, *Angew. Chem. Int. Ed.* **2011**, *50*, 1648; *Angew. Chem.* **2011**, *123*, 1686.
- [23] R. Atkin, P. Davies, J. Hardy, B. Vincent, *Macromolecules* **2004**, *37*, 7979.
- [24] H. C. Shum, D. Lee, I. Yoon, T. Kodger, D. A. Weitz, *Langmuir* **2008**, *24*, 15.
- [25] C. Miesch, I. Kosif, E. Lee, J. Kim, T. P. Russell, *Angew. Chem. Int. Ed.* **2012**, *51*, 145; *Angew. Chem.* **2012**, *124*, 149.
- [26] S. S. Lee, A. Abbaspourrad, S. H. Kim, *ACS Appl. Mater. Interfaces* **2014**, *6*, 1294.
- [27] M. Bendová, K. Rehak, J. Matouš, J. P. Novák, *J. Chem. Eng. Data* **2001**, *46*, 6.
- [28] S. M. Joscelyne, G. Tragardh, *J. Membr. Sci.* **2000**, *169*, 1.
- [29] L. L. A. Adams, T. E. Kodger, S. H. Kim, H. C. Shum, T. Franke, D. A. Weitz, *Soft Matter* **2012**, *8*, 41.
- [30] V. N. Manoharan, M. T. Elsesser, D. J. Pine, *Science* **2003**, *301*, 483.
- [31] S. S. Datta, S.-H. Kim, J. Paulose, A. Abbaspourrad, D. R. Nelson, D. W. Weitz, *Phys. Rev. Lett.* **2012**, *109*, 134302.